GENERALIZED ADAPTIVE RADAR SIGNAL PROCESSING

Paul D. Mountcastle[§], Nathan A. Goodman[¶] and Charles J. Morgan[§]

[§] Technology Service Corporation
Trumbull, CT, 06611

[¶] ECE Dept., University of Arizona
Tucson, AZ, 85721

ABSTRACT

In this paper [1], the use of adaptive weights over the radar measurement dimensions of pulse time, antenna receive element, and wideband frequency is extended to cover a much broader range of radar detection problems than was supposed in the original formulation of space-time adaptive signal processing (STAP). These problems include, among others (1) Adaptive beamforming in three dimensions; (2) Detection and 3D ISAR imaging of targets in general torque-free motion immersed in a field of tumbling clutter dipoles; (3) Detection of moving targets in stationary clutter using all three components of velocity and all three components of position; (4) Discrimination of accelerating targets from uniformly moving targets and stationary clutter; and (5) Adaptive signal processing with distributed and moving array elements. The unifying thread among these applications is the use of adaptive weights over the measured radar data to enhance scatterers that follow one class of paths while suppressing scatterers that follow paths not in that class. Applications (1) and (2) above are treated as examples.

1. INTRODUCTION

The concept of space-time adaptive radar was first introduced as a technique for airborne clutter suppression by Brennan and Reed of TSC in their seminal 1973 paper (Brennan and Reed, 1973). The basic problem was how best to use a linear phased-array receive antenna attached to an airborne radar platform to detect moving targets, while suppressing the strong return from stationary ground clutter. It was recognized by these authors that stationary clutter could be strongly suppressed only by exploiting the correlation between the Doppler shift, as indicated by the phase progression of the radar echo across pulses, with the angle off the array antenna, as indicated by the phase progression of the radar echo across receive elements. A novel criterion was developed by which complex weights over the radar measurement dimensions could be calculated based on the measured radar data. These weights were chosen to satisfy an optimum detection criterion that reduced to inverting a certain complex matrix formed from the radar data.

In this paper, the use of adaptive weights over the radar measurement dimensions of pulse time, antenna receive element, and wideband frequency is extended to cover a much broader range of radar detection problems than was supposed in the original formulation of space time adaptive signal processing (STAP) (Brennan and Reed 1973, Ward 1994). These problems include, among others (1) Adaptive beamforming in three dimensions; (2) Detection and 3D ISAR imaging of targets in general torque-free motion immersed in a field of tumbling clutter dipoles; (3) Detection of moving targets in stationary clutter using all three components of velocity and all three components of position; (4) Discrimination of accelerating targets from uniformly moving targets and stationary clutter; and (5) Adaptive signal processing with distributed and moving array elements. The unifying thread among all applications is the use of adaptive weights over the measured radar data to enhance scatterers that follow one class of paths while suppressing scatterers that follow paths not in that class. These paths are defined in a generalized coordinate system appropriate to the application, and classes are defined according to a conditional probability density function in the path space. These concepts generalize the original problem of separating stationary and linearly moving targets using adaptive weights, and suggest a number of entirely new applications.

In this paper, we show that the calculation of adaptive weights can be formulated without introducing any restrictive assumptions about the space-time configuration of the array elements, and without limiting the classes of paths to uniform linear motion. The adaptive criterion for determining the weights over pulse time, element and wideband frequency is derived from Bayes rule by optimizing the probability of detecting a target of one generalized motion class in the measured radar data while suppressing detection of targets in the other classes, the detection classes being defined by class-conditional probability densities over the entire space of possible paths, called the path space. The result is a matrix optimization problem based on the generalized Rayleigh quotient.

[1] This work was sponsored by the US Army Space and Missile Defense Command and the Missile Defense Agency under STTR contract HQ0006-07-C-7661.

Report Documentation Page

Form Approved
OMB No. 0704-0188

1. REPORT DATE	2. REPORT TYPE	3. DATES COVERED
01 DEC 2008	**N/A**	**-**

4. TITLE AND SUBTITLE	5a. CONTRACT NUMBER
Generalized Adaptive Radar Signal Processing	5b. GRANT NUMBER
	5c. PROGRAM ELEMENT NUMBER
6. AUTHOR(S)	5d. PROJECT NUMBER
	5e. TASK NUMBER
	5f. WORK UNIT NUMBER
7. PERFORMING ORGANIZATION NAME(S) AND ADDRESS(ES) **Technology Service Corporation Trumbull, CT, 06611**	8. PERFORMING ORGANIZATION REPORT NUMBER
9. SPONSORING/MONITORING AGENCY NAME(S) AND ADDRESS(ES)	10. SPONSOR/MONITOR'S ACRONYM(S)
	11. SPONSOR/MONITOR'S REPORT NUMBER(S)

12. DISTRIBUTION/AVAILABILITY STATEMENT
Approved for public release, distribution unlimited

13. SUPPLEMENTARY NOTES
See also ADM002187. Proceedings of the Army Science Conference (26th) Held in Orlando, Florida on 1-4 December 2008

14. ABSTRACT

15. SUBJECT TERMS

16. SECURITY CLASSIFICATION OF:			17. LIMITATION OF ABSTRACT	18. NUMBER OF PAGES	19a. NAME OF RESPONSIBLE PERSON
a. REPORT **unclassified**	b. ABSTRACT **unclassified**	c. THIS PAGE **unclassified**	**UU**	**7**	

In Section 2, we present the ideas of generalized coordinates, path space, and classes in path space. These concepts unify the mathematics for various applications. We then derive the algorithm for calculating adaptive weights. In Section 3, we present simulated results for two different applications. The first is a demonstration of beamforming using a distributed antenna array. The beamforming problem can be viewed as a case of the general theory in which a scatterer path is uniquely determined by its position in some fixed reference frame, meaning that all the scatterers of interest are stationary. A region of space is selected in which scatterers should be enhanced and a different region is selected in which scatterers should be suppressed. Next, we consider the problem of various objects moving in general states of torque-free motion in the presence of large numbers of tumbling clutter dipoles (Cuomo et al 1999, Mayhan et al 2001). Here, the distinguishing characteristic of the clutter scatterers is that they move uniformly along circles in space while the target object precesses and spins.

2. THEORY OF GENERALIZED ADAPTIVE RADAR SIGNAL PROCESSING

We now develop an extension of the theory of adaptive radar that combines the concepts of STAP and radar imaging. The result is a scheme for separating scatterers that move according to one class of space-time trajectories from scatterers that move according to another class of trajectories or paths. These paths are readily visualized through motion-invariant generalized coordinates called the path space. The introduction of generalized coordinates admits many applications including detection of moving targets in stationary ground clutter using three velocity components, three position components, and netted radar; and detection and 3D imaging of targets undergoing general torque-free motion immersed in a field of tumbling clutter dipoles.

2.1 Phase Histories in Generalized Coordinates

Let the symbol q represent the set of parameters that describe the path a particular scatterer takes over time. Since q defines a space-time path, we refer to q as the scatterer's *generalized coordinates*. Several examples of generalized coordinates include:

- For stationary scatterers, q is the three-dimensional position vector $\mathbf{x}$, which describes the scatterer position at all times;
- For scatterers in linear motion, $q = (\mathbf{x}_0, \mathbf{v})$ is a six-dimensional vector comprised of the scatterer's position $\mathbf{x}_0$ at some reference time and the three-dimensional velocity vector $\mathbf{v}$;
- For scatterers attached to a rigid body in torque-free motion, $q = (\boldsymbol{\Omega}, \mathbf{s}_b)$ is comprised of motion parameters $\boldsymbol{\Omega}$ and a position vector $\mathbf{s}_b$. The vector $\boldsymbol{\Omega}$ contains six parameters to describe the motion of the body's center of mass as well as parameters that describe the motion of the body's principal axes in space. The vector $\mathbf{s}_b$ describes the position of the scatterer relative to the principal axes of the rigid body.

Let the space-time position of a scatterer throughout the coherent dwell be written symbolically as $\mathbf{x}(t \mid q)$ where t is a pulse time. The generalized multistatic data cube is also defined as $z(f, e, t)$, where f is a wideband frequency and e is the index of a receive element. Thus the quantity z is the raw measured radar data, sometimes called I&Q data, collected during a coherent processing interval (CPI) over (possibly) several receive elements. The geometry-dependent signal phase due to the scatterer is

$$\phi(q, f, e, t) = -\frac{2\pi f}{c}\left\{\left|\mathbf{T}(t) - \mathbf{x}(t \mid q)\right| + \left|\mathbf{R}(e, t) - \mathbf{x}(t \mid q)\right|\right\} \quad (1)$$

where $\mathbf{T}(t)$ denotes the radar transmitter trajectory throughout the coherent dwell and $\mathbf{R}(e, t)$ denotes the trajectory of the "eth" receive element.

Next, a *class of paths* C is defined by specifying a class-conditional probability density $p(q|C)$ in the space q of generalized coordinates, which we may call the path space. These class-conditional probability densities in path space provide a unified formal language by means of which the radar designer can precisely specify any number of signal and interference classes on the basis of physical features of the postulated scatterer motions, independent of the description of the radar measurement. The design technique has broad applications to 3D adaptive beamforming, six-dimensional (position plus velocity) air- and ground-moving target detection, three-dimensional adaptive ISAR with one or more radars and many other problems. The goal of the adaptive process is to design window functions that selectively image scatterers belonging to one class, denoted C, while suppressing scatterers belonging to any other classes (collectively denoted C'). The designer has the freedom to define any number of such classes.

2.2 Adaptive Algorithm

The complex quantity

$$\Phi(z, q, w) = \sum_t \sum_f \sum_e w(f, e, t)\, z(f, e, t) \exp\left[-i\phi(q, f, e, t)\right] \quad (2)$$

admits the interpretation of the complex amplitude corresponding to the presence of a scatterer following the

path q in the w-filtered data cube z. Let the adaptive weights corresponding to a particular class C of scatterers be $w(C)$. The correspondence between the window and the class is intended to imply that the image viewed through the window $w(C)$ should show scatterers in q-space whose motions belong to class C but suppress scatterers whose motions correspond to other classes (collectively, C'). It is convenient to introduce the Dirac 'bra' and 'ket' symbols for complex row and column vectors (Dirac 1981, Shankar 1994). Using this notation, we introduce the column vector $|q,z\rangle$ of dimension $n_f\, n_e n_t \times 1$. The nth element of the vector is the nth sample of the data cube (ordered in any convenient way), phase-corrected according to the phase history of a scatterer following path q. That is, the elements of $|q,z\rangle$ are

$$\langle q,z|_{f,e,t} = z(f,e,t)\exp\left[-i\phi(q,f,e,t)\right]. \tag{3}$$

The dual labels q and z in the symbol on the left-hand side of (3) indicate that the vector depends both on the model, through q, and the data, through z. We will use the shorthand symbol $|q\rangle$ to indicate this vector in the remainder of this paper wherever no confusion is likely to arise, but the dependence of the quantity on the measured data z should be borne in mind. Indeed, it is through this dependence on the measured data that the algorithm to be developed can be said to be adaptive. Similarly, we define $\langle w(C)|$ as the class-conditioned adaptive weights rearranged into row vector form. Hence, (2) is now denoted

$$\Phi(z,q,w) = \langle w(C)|q,z\rangle. \tag{4}$$

We will likewise omit the reference to the particular class C (for brevity) and simply write $|w\rangle$ when no confusion is likely to arise. Nonetheless, it should be remembered that there will be a separate weight vector for each class. Finally, we define the likelihood that a scatterer following path q is present in the measured data z as the normalized power in the C-filtered image

$$p(z\,|\,q,C) = \langle w(C)|q,z\rangle\langle q,z|w(C)\rangle. \tag{5}$$

This is consistent with the standard definition of likelihood (Sivia 2006) as long as the required normalization is absorbed into the adaptive weights, i.e. $\langle w|w\rangle = 1$. The brighter the image of a particular path in the path-space q, the more likelihood we assign to the proposition that a scatterer following that path is present. These statements are sufficient to qualify the normalized power $|\langle q|w\rangle|^2 = \langle w|q\rangle\langle q|w\rangle$ in the filtered image as a likelihood in the standard definition and formal notation (Cox 1961).

The adaptive weights are determined by the condition that the probability of a scatterer of class C given the radar measurement z is a maximum. The quantity that must be maximized by the choice of weights $|w(C)\rangle$ is the probability of class C conditioned on the data z, denoted by $P(C|z)$. We can apply the rules of probability theory to express this in terms of the suitably marginalized joint distribution, $p(C,z,q)$, according to

$$P(C|z) = \frac{\int dq\, p(q,z,C)}{\sum_{C'}\int dq\, p(q,z,C')}. \tag{6}$$

The summation in the denominator is over all classes, and the integrations are over distinct sets of motion parameters. The joint distribution $p(C,z,q)$ can be factored by applying the product rule for probabilities. Specifically, the joint distribution of two propositions π_1 and π_2 can be expanded by the product rule as

$$p(\pi_1,\pi_2) = p(\pi_1)\,p(\pi_2\,|\,\pi_1). \tag{7}$$

In order to expand $p(C,z,q)$, we let $\pi_1 = C$ and $\pi_2 = z\,q$. Then, two successive applications of the product rule give

$$p(C,z,q) = p(C)\,p(q\,|\,C)\,p(z\,|\,q,C). \tag{8}$$

Therefore, substituting (8) into (6), we obtain

$$P(C|z) = \frac{p(C)\int dq\, p(q\,|\,C)\,p(z\,|\,q,C)}{\sum_{C'} p(C')\int dq\, p(q\,|\,C')\,p(z\,|\,q,C')}. \tag{9}$$

Finally, we use the definition of $p(z\,|\,q,C)$ in (5) as the normalized C-filtered image power in path-space. The weights are taken to the outside of the sums and integrals, expressing the inner products in the numerator and denominator of (9) in the form $\langle w\,|\,\boldsymbol{\theta}\,|\,w\rangle$, where $\boldsymbol{\theta}$ denotes a square matrix. This gives

$$P(C|z) = \frac{\langle w|\left[\int dq|q\rangle\, p(C)\,p(q\,|\,C)\langle q|\right]|w\rangle}{\langle w|\left[\sum_{C'}\int dq|q\rangle\, p(C')\,p(q\,|\,C')\langle q|\right]|w\rangle}. \tag{10}$$

We wish to find the weights $|w(C)\rangle$ that maximize (10). Therefore, the solution to finding the adaptive weights consists of three steps:

1. *Define* the classes of motion to be separated in a path space of generalized coordinates q by specifying a set of class-conditional probability densities $p(q|C)$;

2. *Compute* the class-specific matrices **A** and **B** from the specified motion class definitions and the measured coherent radar data z according to

$$\begin{aligned}\mathbf{A} &= \int dq |q\rangle P(C)\, p(q|C) \langle q| \\ \mathbf{B} &= \sum_{C'} \int dq |q\rangle P(C')\, p(q|C') \langle q|\end{aligned}; \tag{11}$$

3. *Solve* the variational problem

$$\delta\left[\frac{\langle w|\mathbf{A}|w\rangle}{\langle w|\mathbf{B}|w\rangle}\right] = 0\,. \tag{12}$$

The quantity to be maximized is a quotient of quadratics of a kind that has been studied extensively in connection with applications of the Rayleigh-Ritz variational principle of quantum mechanics, and also in the context of the finite element method (Strang 1988). The solution weight vector is the largest eigenvector associated with the two-operator eigenvalue problem

$$\mathbf{A}|w\rangle = \lambda \mathbf{B}|w\rangle\,. \tag{13}$$

While the primary eigenvector of (13) will maximize the ratio (12), other eigenvectors may also be useful. In fact, the primary eigenvector likely will not span the entire q-space of the desired class, and more eigenvectors will be needed to image all the paths in the desired class. This property will be addressed in the next section where we demonstrate the ability of our adaptive algorithm.

3. SIMULATION RESULTS

We now demonstrate the ability of the above adaptive algorithm to image scatterers following a desired class of paths while rejecting other scatterers following undesired paths. We begin with a demonstration where scatterers are imaged or suppressed based only on their position. In this demonstration, the radar measurements are collected over many radar locations randomly distributed in the far field around the plane being imaged. In the second demonstration, we use the generalized coordinates to define two classes – one for a fixed body in torque-free motion and another for tumbling clutter dipoles. We show that the dipoles can be suppressed while successfully imaging scatterers on the fixed body.

The simplest example of a path space is one in which all of the scatterers are stationary in a particular frame so that the three-dimensional vector **x** relative to that frame is sufficient to specify the trajectory of any scatterer throughout the coherent interval. This corresponds to the first example of generalized coordinates in the list from Section 2. The problem of detecting scatterers in certain regions of space while suppressing scatterers in other regions of space is an extension of the idea of beamforming. At the same time, it is the simplest nontrivial example of the generalized adaptive theory.

3.1 Demonstration of Adaptive Beamforming (2D)

In this demonstration, approximately 122 scatterers were distributed over a square planar surface measuring 1.2m per side. The first 100 scatterers were distributed randomly while the next 22 scatterers were arranged in a letter 'A' (for Arizona). 750 radar elements were randomly distributed in angle around the scattering surface. The elements were in the same plane as the scatterers and were located in the far field of the scattering surface. The frequency of operation was chosen to be 3 GHz.

The path-space classes were defined as follows. Several sub-regions within the 1.2m × 1.2m image plane were assigned to the "desired" class C. These sub-regions sampled the outline of the letter 'A', and any point q = **x** within 0.04m of the center of a sub-region was defined as a member of the desired class. All points located greater than 0.04m away from the center of these sub-regions were assigned to the undesired class C'. This setup tests the adaptive algorithm's ability to compute a window function that passes scatterers located in the sub-regions but reject scatterers outside the sub-regions.

For each class, the **A** and **B** matrices were computed numerically. For uniformly distributed points within each path space, the phase history $\phi(q,e)$ of a scatterer at each point was calculated. Then, the "steering vectors" $\mathbf{a}_q = \exp\left[i\phi(q,e)\right]$ were computed, and the matrices **A** and **B** were calculated according to

$$\mathbf{A} = \sum_{\mathbf{q}\in C} \mathbf{a}_q \mathbf{a}_q^{\mathrm{H}} \tag{14}$$

$$\mathbf{B} = \sum_{\mathbf{q}\in C'} \mathbf{a}_q \mathbf{a}_q^{\mathrm{H}}\,. \tag{15}$$

Figures 1-4 show the results from this experiment. First, Figure 1 shows the image that results from direct correlation-based processing without adaptive windowing. As one can see from the figure, energy is distributed throughout the image area. Figure 2 shows the image that results from the adaptive algorithm described above using only the primary eigenvector of the generalized eigenvalue problem defined by **A** and **B**. Although several

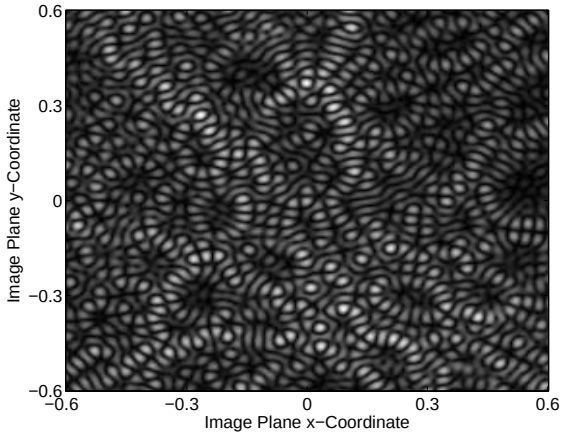

Fig. 1. Image of scattering plane using non-adaptive correlation (matched filtering).

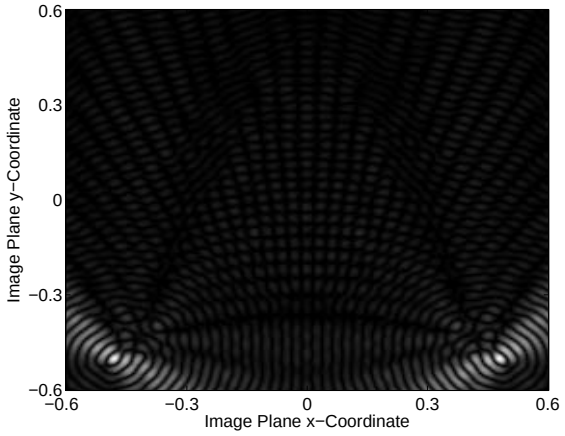

Fig. 2. Image of scattering plane using principal eigenvector as the adaptive weights.

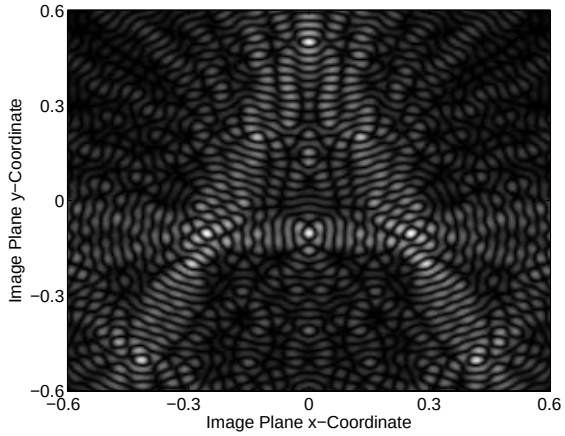

Fig. 3. Image of scattering plane using third eigenvector as the adaptive weights.

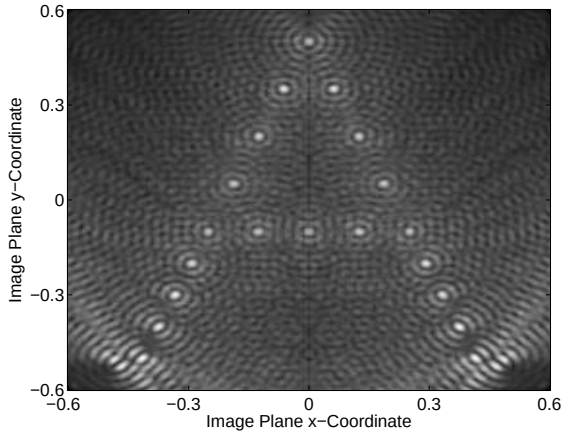

Fig. 4. Image formed by adding (in magnitude) images formed from the first 22 eigenvectors.

sub-regions of the image plane were assigned to the desired class, the image in Figure 2 shows energy highly concentrated into only two locations. These were the two regions contained within class *C* that had the most scattering energy and, therefore, were the most important regions to be represented by the first eigenvector.

Figure 3 shows the image that results from using only the third eigenvector. This image shows energy from the other sub-regions of path space assigned to class *C*. Finally, Figure 4 shows the result when images are formed from each of the first 22 eigenvectors, and then summed together (in magnitude). The image in Figure 4 clearly shows the letter 'A' that was outlined by the definition of the desired class *C*.

3.2 Torque-Free Objects Immersed in Clutter

In this demonstration, we show the ability to suppress clutter scatterers modeled as dipoles in a tumbling motion from a target object in a different motion state. Both the target and clutter dipoles are located within the same 1.5 meter sphere. The system is modeled as having a coherent processing interval (CPI) of 8.5 seconds, a center frequency of 3 GHz and a bandwidth of 300 MHz. The sphere of scatterers is located at the origin of the inertial frame coordinate system while the single radar is located in the sphere's far field.

As mentioned above in Section 2, the generalized coordinates that describe a path in torque-free motion

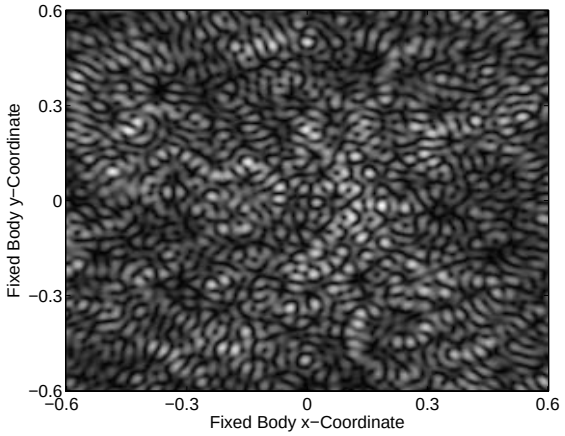

Fig. 5. Image of the base of a cone in torque-free motion immersed in clutter using matched filtering.

include a position vector that describes a scatterer's position in a coordinate frame fixed to the rigid body. The generalized coordinates also include parameters that describe the motion of the fixed body's center of mass, as well as motion parameters that describe the motion of the fixed body's coordinate frame relative to an inertial coordinate frame.

Let the generalized coordinates of a scatterer located on a fixed body in torque-free motion be denoted as in Section 2 by $q = (\mathbf{\Omega}, \mathbf{s}_b)$. The time-varying position of the scatterer in Earth-centered inertial coordinates is

$$\mathbf{x}(t) = \mathbf{c}_g(t) + [\mathrm{E\ B}](t \mid \mathbf{\Omega})\mathbf{s}_b \qquad (16)$$

where $\mathbf{c}_g(t)$ is the body's time-varying center of mass, and $[E\ B]$ denotes the time-varying orthogonal matrix that transforms vectors in the body reference frame B to vectors in the inertial frame E. If the radar location is defined by the vector **r**, the time-varying range to the scatterer is

$$R(t) = \left|\mathbf{x}(t) - \mathbf{r}\right| = \left|\mathbf{c}_g(t) + [\mathrm{E\ B}](t \mid \mathbf{\Omega})\mathbf{s}_b - \mathbf{r}\right|. \quad (17)$$

When approximated with a first-order Taylor expansion around $\mathbf{s}_b = \mathbf{0}$, the range becomes

$$R(t) \approx R_g(t) + \left([\mathrm{E\ B}](t \mid \mathbf{\Omega})\mathbf{s}_b\right)^{\mathrm{T}} \hat{\mathbf{r}}(t) \qquad (18)$$

where $R_g(t)$ and $\hat{\mathbf{r}}(t)$ are the time-varying range and unit vector from the radar to the object's center of mass, respectively. We assume in our simulations that the directional unit vector changes little during a coherent processing interval allowing us to ignore the time dependence of $\hat{\mathbf{r}}(t)$. We further assume that the data have been range-corrected to remove the delay due to translational motion of the center of mass (Mayhan 2001).

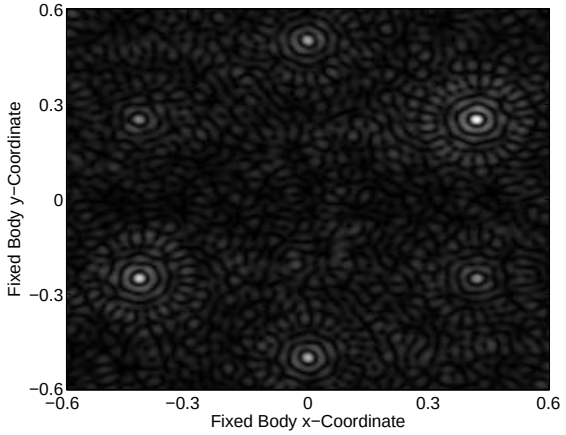

Fig. 6. Image of the base of a cone in torque-free motion immersed in clutter using principal eigenvector as the adaptive weights.

In our experiment, the target is modeled as a cone with six scatterers uniformly placed around the cone's base. The *z*-axis of the fixed body frame passes through the center of the cone's base and runs through the tip of the cone. The *x*-*y* plane of the fixed body frame is parallel to the base of the cone. The tip of the cone wobbles, or precesses, around the inertial *z*-axis, and the cone spins about its own *z*-axis.

Clutter is modeled as a scattering dipole. The scattering from the dipole is assumed to come primarily from both ends. Therefore, the dipole is modeled as two equal scatterers at opposite ends of a fixed axis. The motion of the dipole is precisely an end-over-end motion, though the orientation of the tumbling plane is random. 100 dipoles were randomly placed in the 1.5m-radius sphere with random tumbling orientations. The scattering from a single end of the dipole was about the same RCS as the scattering from one of the target scatterers.

The clutter dipole suppression matrix **B** was calculated in two parts by separating the contributions due to location of the fixed body's center of mass and to the rotational motion of the fixed body's axes in the inertial frame. The component due to the location of the center of mass can be calculated analytically. The component due to rotation motion was calculated numerically by training over scatterers with varying rotational parameters.

To form an image of a rotating target, the image must be referenced to the frame of the fixed body. Therefore, we imaged the base of the cone in fixed body coordinates where the cone scatterers were located. Figure 5 shows the result when the image is formed non-adaptively using straight correlation or matched filtering. One can see in Figure 5 that the presence of dipoles in the same imaging volume has obscured any structure that may correspond to

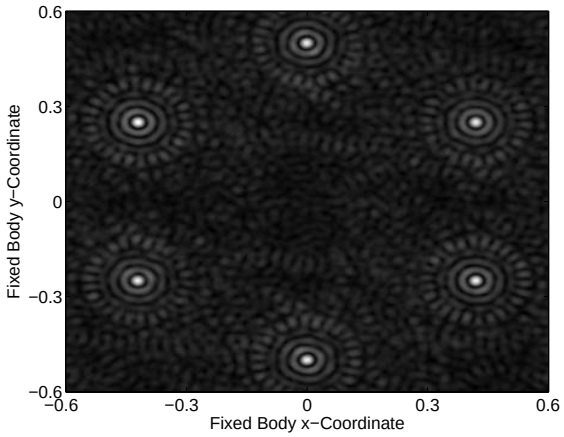

Fig. 7. Image of the base of a cone in torque-free motion immersed in clutter using sum of images from first five generalized eigenvectors.

the base of the cone. Figure 6 shows the result when the adaptive algorithm is applied using only the first eigenvector of the generalized eigenvalue problem. Figure 7 shows the result when the first five eigenvectors are used to generate five images, which are then summed in magnitude. The adaptive weights are clearly able to suppress the dipoles' tumbling motion while imaging scatterers in a different motion state.

4. CONCLUSIONS

We have presented and demonstrated an innovative extension to adaptive signal processing that can be applied to a wide range of circumstances. The new algorithm relies on definitions of desired (target) and undesired (clutter) classes according to their generalized coordinates in path space. The makeup of the generalized coordinates varies with application. In beamforming applications with no scatterer motion the generalized coordinates are simply a position vector in a common reference frame. In applications involving torque-free motion, the generalized coordinates includes descriptions of scatterers in the fixed body's frame of reference, the motion of the body's center of mass, and the motion of the body's frame relative to an inertial frame.

Regardless of the application, the generalized coordinates describe the "path" that a scatterer takes during the radar CPI. Then, the class-conditioned pdf quantifies the likelihood that a scatterer belonging to a certain class would be following a particular path. By interpreting the image that results from windowed/weighted data as a class-conditioned probability density, a probability expression can be derived and used as the objective function in calculating the optimum weight function.

The new adaptive algorithm is very versatile as indicated by the simulation results that were presented. The scenarios that were simulated included both beamforming for stationary scatterers as well as a target object in torque-free motion and immersed in clutter dipoles in different motion states. In both cases, the adaptive algorithm successfully imaged scatterers in the desired class while suppressing scatterers in an undesired class.

REFERENCES

Brennan, L.E. and Reed, I.S., "Theory of Adaptive Radar", *IEEE Transactions on Aerospace and Electronic Systems*, AES-9, no. 2, (March 1973), pp. 237-252.

Cox, R. T., *The Algebra of Probable Inference*, The Johns Hopkins University Press, Baltimore MD, 1961.

Cuomo, K.M., Piou, J.E., and Mayhan, J.T., "Ultrawide-band coherent processing," *IEEE Transactions and Antennas and Propagation*, vol. 47, no. 6, (June 1999), pp. 1094-1107.

Dirac, P.A.M., *The Principles of Quantum Mechanics, 4th Edition*, Clarendon Press, Oxford England, UK, 1981.

Mayhan, J.T., et al, "High resolution 3D "snapshot" ISAR imaging and feature extraction," *IEEE Transactions on Aerospace and Electronic Systems*, vol. 37, no. 2, (April 2001), pp. 630-642.

Shankar, R., *Principles of Quantum Mechanics, 2nd Edition*, Plenum Press, New York, 1994.

Sivia, D. S. and Skilling, J, *Data Analysis: a Bayesian Tutorial*, Oxford University Press, Oxford, 2006.

Strang, G., *Linear Algebra and its Applications, 3rd Edition*, Harcourt Brace and Jovanovich, New York, 1988.

Ward, J., *Space-Time Adaptive Processing for Airborne Radar*, MIT Lincoln Laboratory Technical Report 1015, December 13, 1994.